

Target Illumination by Structured Beam for Advanced Radar Scattering Analysis

Kobe Prior and Atef Elsherbeni

kdprior@mines.edu ; aelsherb@mines.edu

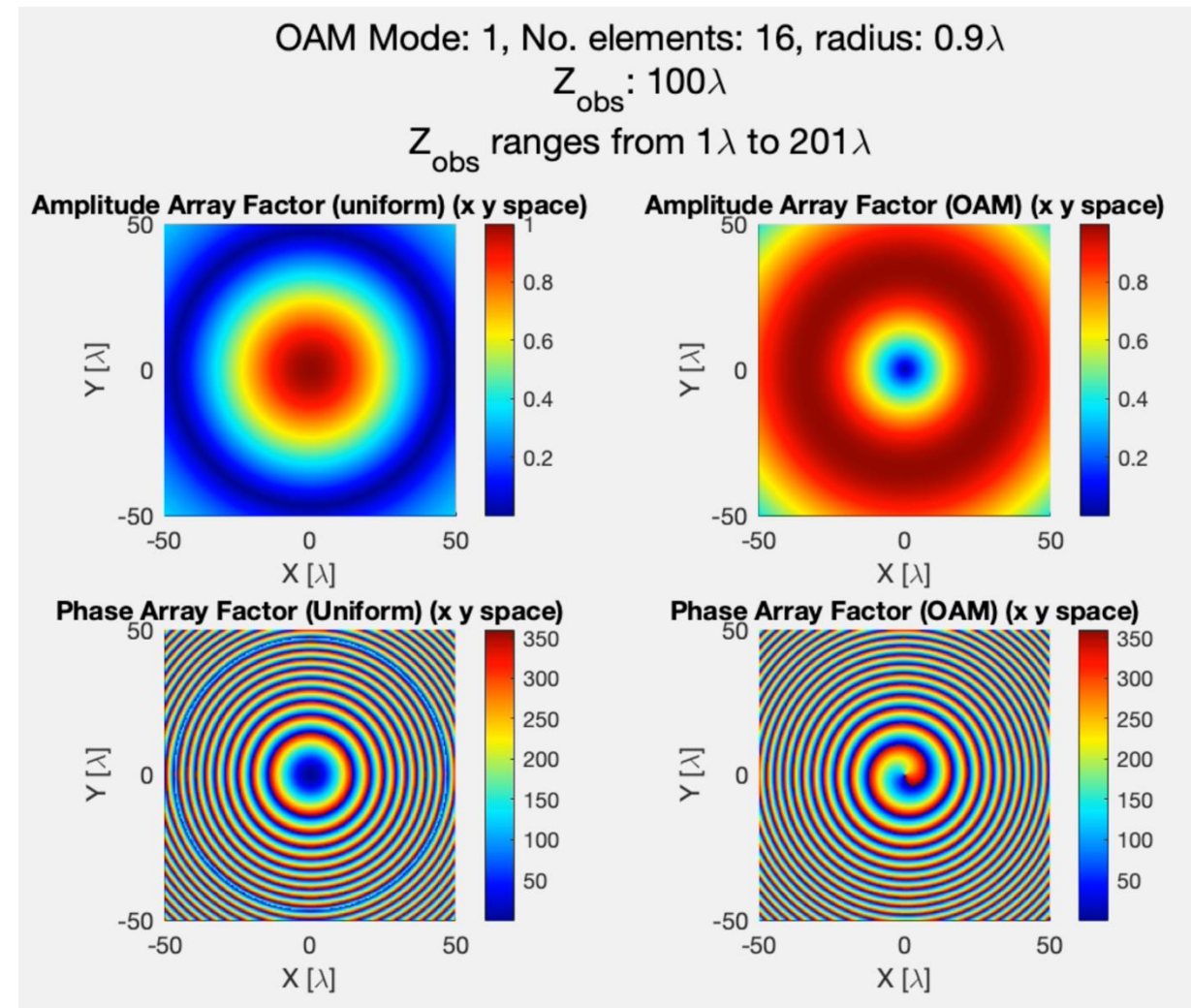


Outline

- Background and Motivation
- Generating Beams with Orbital Angular Momentum
- Simulation
 - Methodology
 - Results
 - Plane Wave Illumination
 - Structured Beam Illumination
- Phased Array System Design
 - System Overview
 - Measurement Setup
- Comparison of Results
- Conclusion
- Future Work

Background and Motivation

- Structured beams are a class of waveforms that propagate with spatial variation in phase and amplitude
- The specific class of beams this research explores are waveforms carrying Orbital Angular Momentum (OAM)
- Traditional radar systems use plane waves to illuminate targets so by implementing structured beams an additional degree of freedom is unlocked
- Before radar systems can fully utilize structured beams careful characterization of scattering interactions must be performed.



Generating Beams with Orbital Angular Momentum

To generate beams that carry orbital angular momentum using antenna arrays the Laguerre-Gaussian Vector Beam Expression is used to synthesize the phase each element is excited with.

$$E_p^l(r, \phi, z) = \underbrace{\frac{1}{w(z)} \sqrt{\frac{2p!}{\pi(p+|l|)!}}}_{\text{Normalization}} \underbrace{\left(\frac{\sqrt{2}r}{w(z)}\right)^{|l|}}_{\text{Azimuthal amplitude dependence}} \underbrace{L_p^{|l|}\left(\frac{2r^2}{w(z)^2}\right)}_{\text{Generalized Laguerre polynomial}}$$

$$\times \underbrace{\exp\left(-\frac{r^2}{w(z)^2}\right)}_{\text{Gaussian envelope}} \underbrace{\exp\left(-j\frac{kr^2}{2R(z)}\right)}_{\text{Wavefront curvature (focusing)}} \underbrace{\exp(-jl\phi)}_{\text{OAM helical phase}} \underbrace{\exp(j\psi(z))}_{\text{Gouy phase}}$$

$r = \sqrt{x^2 + y^2}$ (Radial coordinate)

$\phi = \tan^{-1}\left(\frac{y}{x}\right)$ (Azimuthal angle)

$k = \frac{2\pi}{\lambda}$ (Wavenumber)

$z_R = \frac{\pi w_0^2}{\lambda}$ (Rayleigh range)

$w(z) = w_0 \sqrt{1 + \left(\frac{z}{z_R}\right)^2}$ (Beam radius at z)

$R(z) = z \left(1 + \frac{z_R^2}{z^2}\right)$ (Radius of curvature)

$\psi(z) = (|l| + 2p + 1) \tan^{-1}\left(\frac{z}{z_R}\right)$ (Gouy phase)

$L_p^{|l|}(x) = \frac{e^x x^{-|l|}}{p!} \frac{d^p}{dx^p} (e^{-x} x^{p+|l|})$ (Generalized Laguerre polynomial)

(Radial coordinate)

(Azimuthal angle)

(Wavenumber)

(Rayleigh range)

(Beam radius at z)

(Radius of curvature)

(Gouy phase)

(Generalized Laguerre polynomial)

where l is the angular mode number, p is the radial mode number

To synthesize this beam using an antenna array the assignment of the phase at each antenna port is determined by evaluating the phase of the LG expression at the antenna position $\angle E_p^l(r = r_{\text{element}}, \phi = \phi_{\text{element}}, z = z_0)$

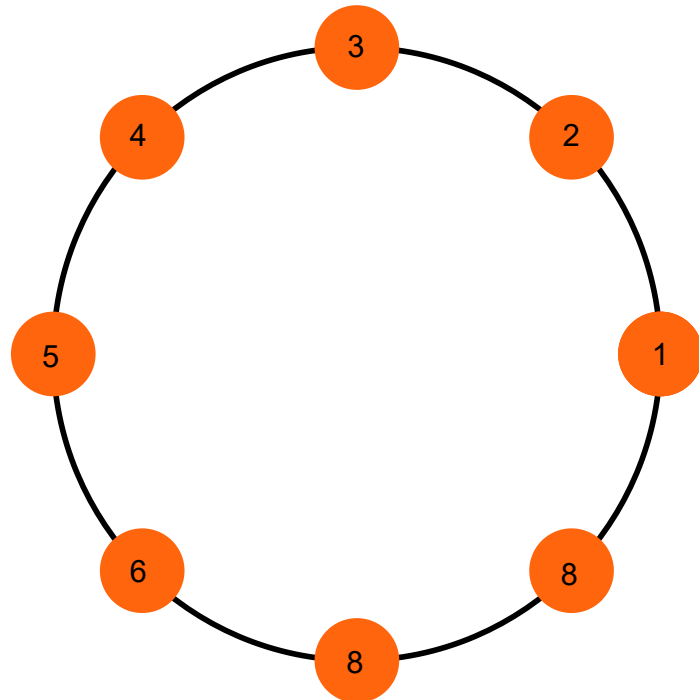
Generating Beams with Orbital Angular Momentum

Asserting uniform amplitude excitation, no focusing, and radial mode number $p = 0$ we arrive at an expression for the electric field of an OAM vortex mode:

$$E_0^l(r, \phi, z) \propto E_0 e^{jkz} e^{jl\phi}$$

Thus, generating beams carrying orbital angular momentum is achieved by applying a phase shift to an element equivalent to the mode number l multiplied by the azimuthal position of the element.

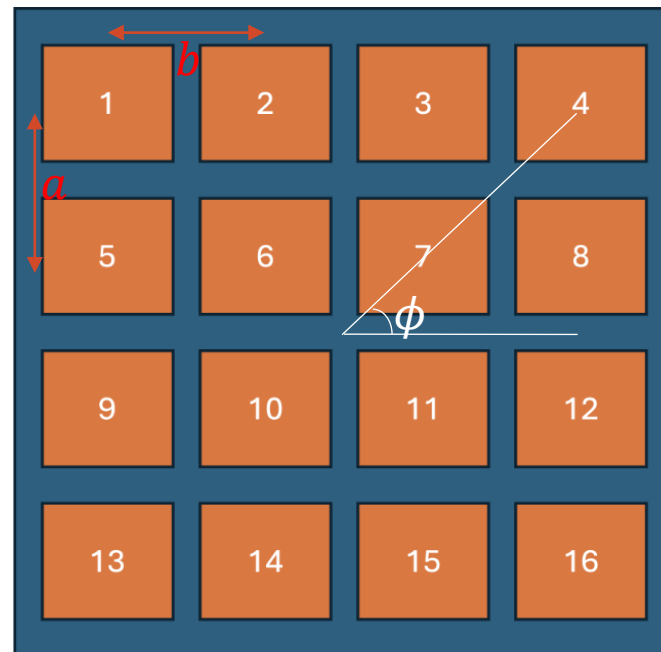
Uniform Circular Array



$l = 1$

Element	Phase
1	0°
2	45°
3	90°
4	135°
5	180°
6	225°
7	270°
8	315°

Rectangular Antenna Array



$l = 1, a = 48.3 \text{ mm}, b = 56.4 \text{ mm}$

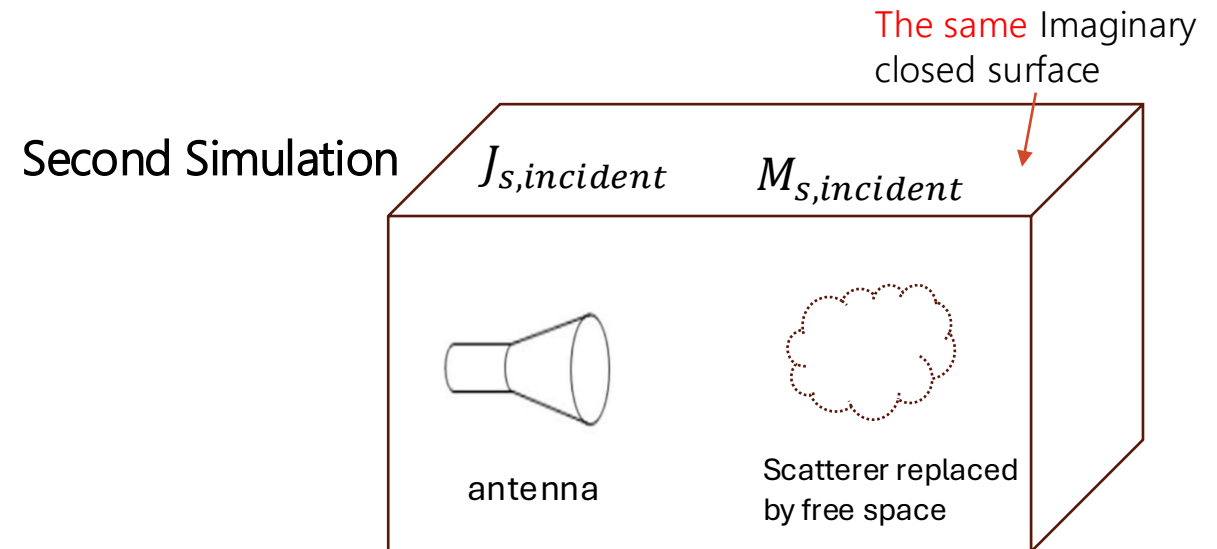
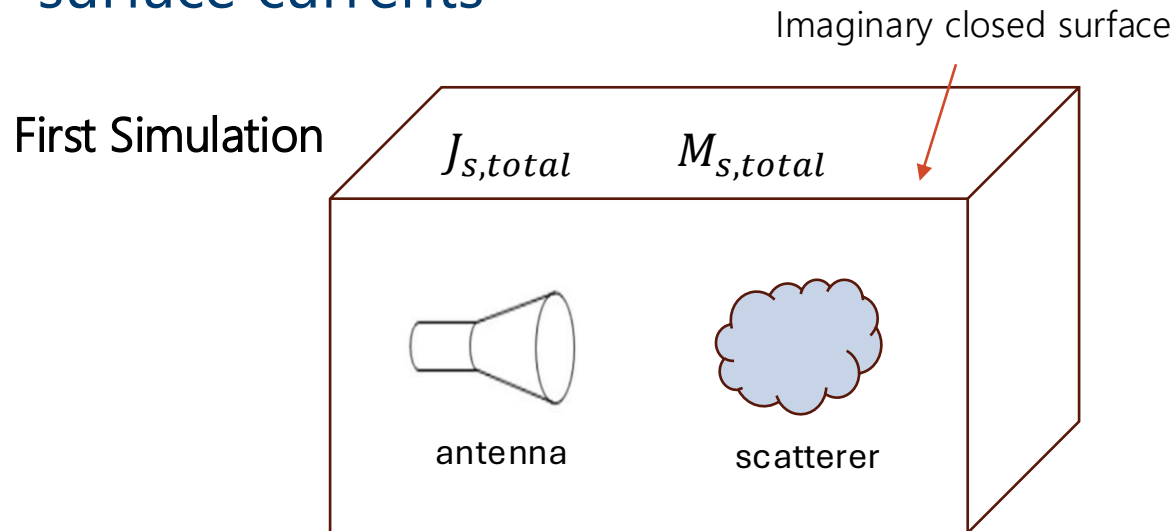
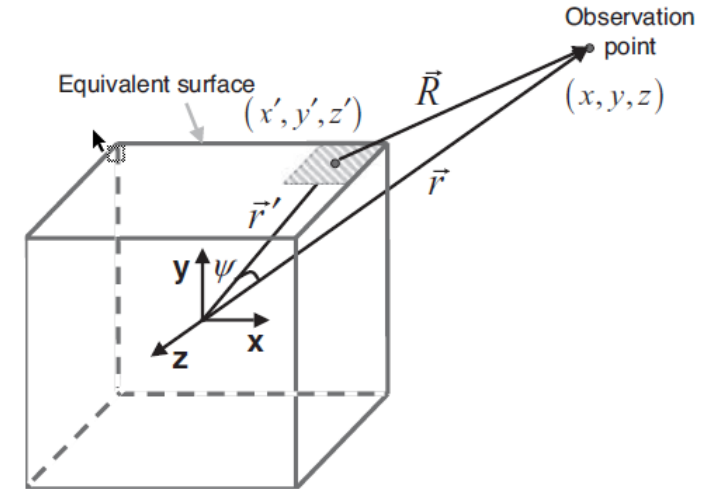
Element	Phase	Element	Phase
1	130.6°	9	201.3°
2	105.9°	10	229.4°
3	74.1°	11	310.6°
4	49.4°	12	338.7°
5	158.7°	13	229.4°
6	130.6°	14	254.1°
7	49.4°	15	285.9°
8	21.3°	16	310.6°

Simulation: Methodology

- Two fictitious surface currents (electric and magnetic) are computed on the boundary of a simulation domain
- If these are computed with a scatterer and without a scatterer, we can isolate the scattering by subtracting the surface currents

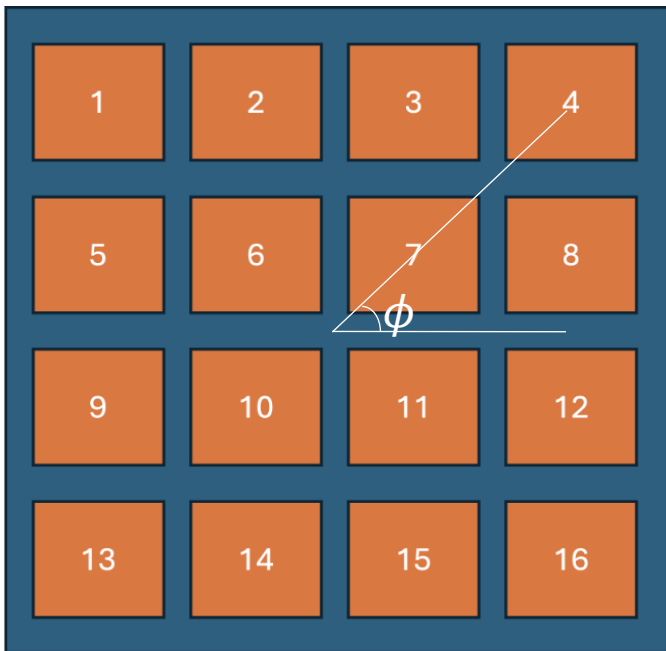
$$J_{s,scattered} = J_{s,total} - J_{s,incident} \quad M_{s,scattered} = M_{s,total} - M_{s,incident}$$

- Then scattered far fields can be computed from the resulting surface currents

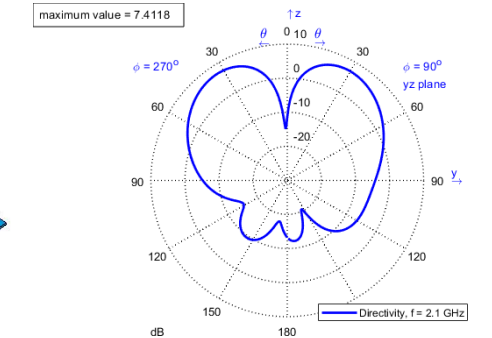
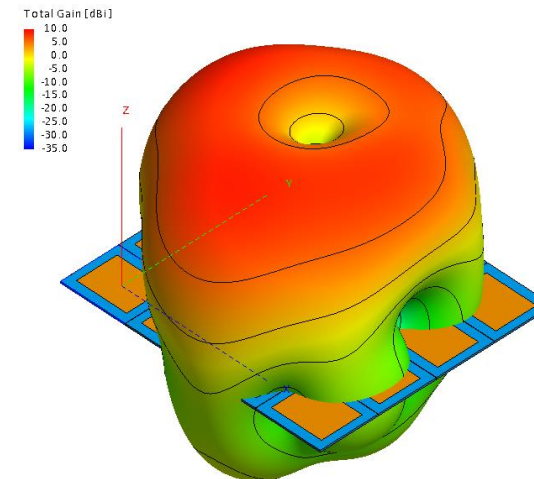
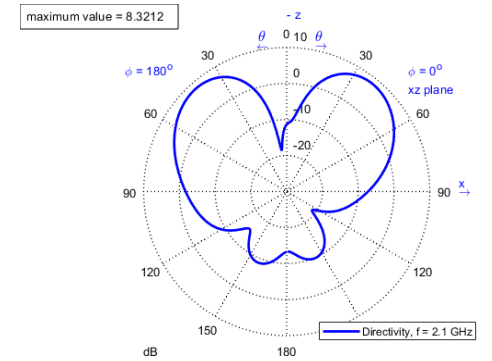
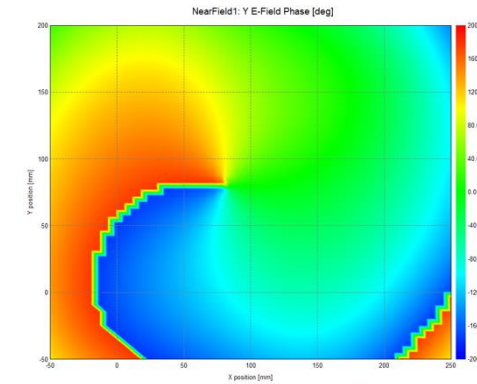


Simulation Results – Rectangular Array

For the physical implementation, a rectangular array is used with an operating frequency of 2.1 GHz. Simulation is conducted using the FDTD solver in CEMS and the MoM solver in FEKO. With the shown assigned phase excitation, results yield the expected radiation pattern and electric field phase distribution.

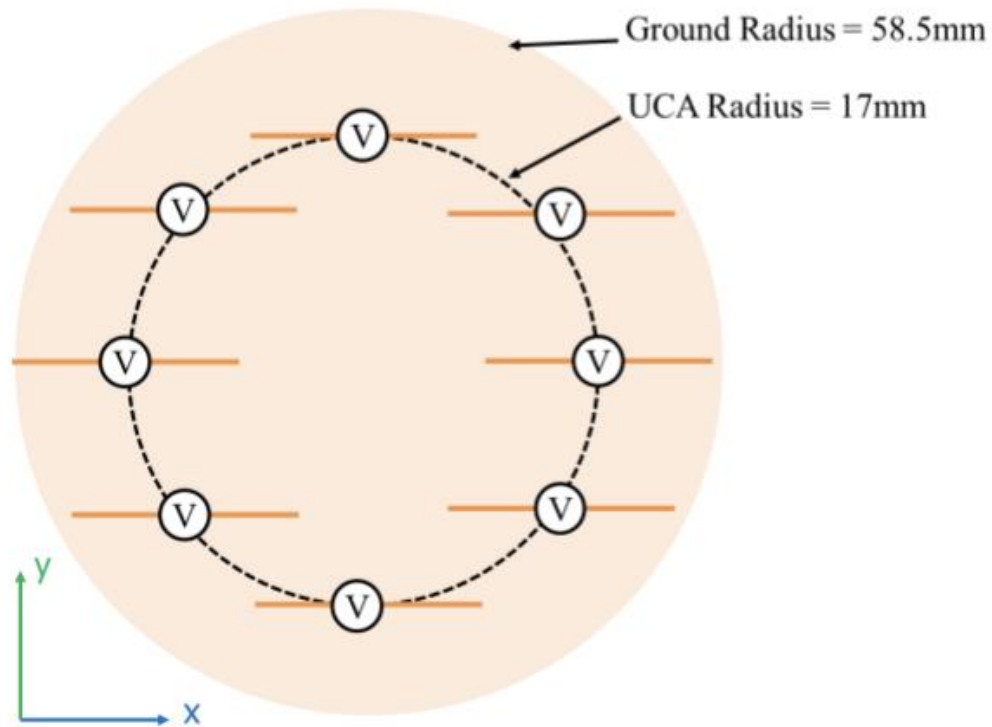


Element	Phase	Element	Phase
1	130.6°	9	201.3°
2	105.9°	10	229.4°
3	74.1°	11	310.6°
4	49.4°	12	338.7°
5	158.7°	13	229.4°
6	130.6°	14	254.1°
7	49.4°	15	285.9°
8	21.3°	16	310.6°



Simulation Results – Circular Array

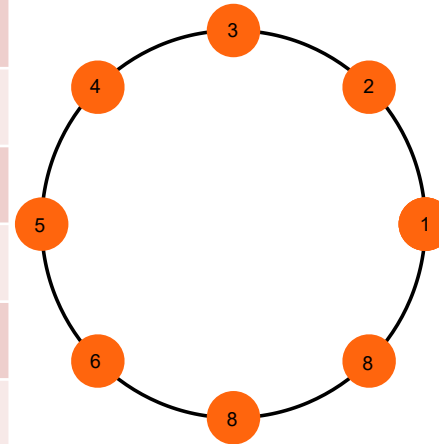
To simplify the simulation domain for scattering analysis a uniform circular array of dipole antennas backed by a planar reflector operating at 8.75 GHz is used



The far field boundary is defined by $z_{ff} = \frac{2D^2}{\lambda} \approx 200 \text{ mm}$

$l = 1$ (OAM)

Element	Phase
1	0°
2	45°
3	90°
4	135°
5	180°
6	225°
7	270°
8	315°



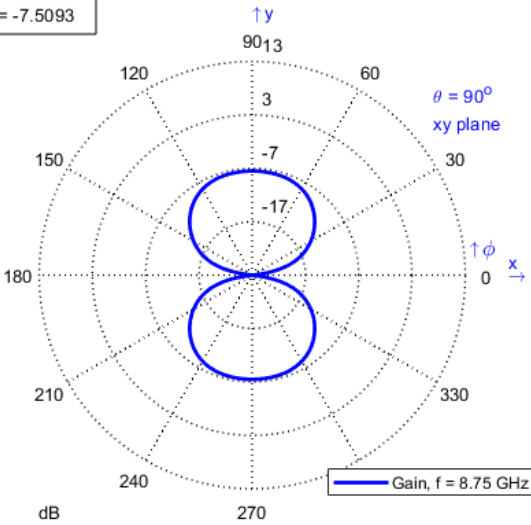
$l = 0$ (planewave)

Element	Phase
1	0°
2	0°
3	0°
4	0°
5	0°
6	0°
7	0°
8	0°

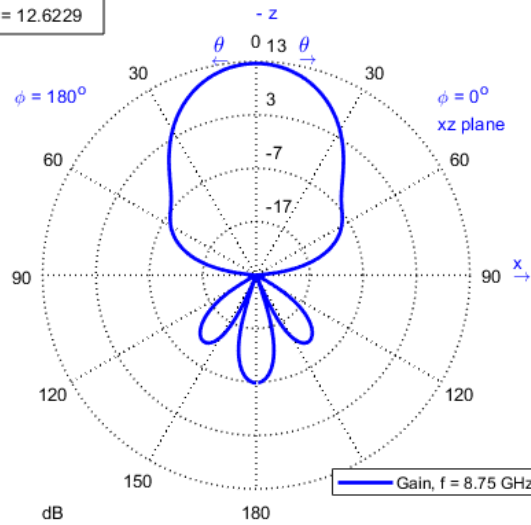
Circular Array Radiation Characteristics

OAM mode 0

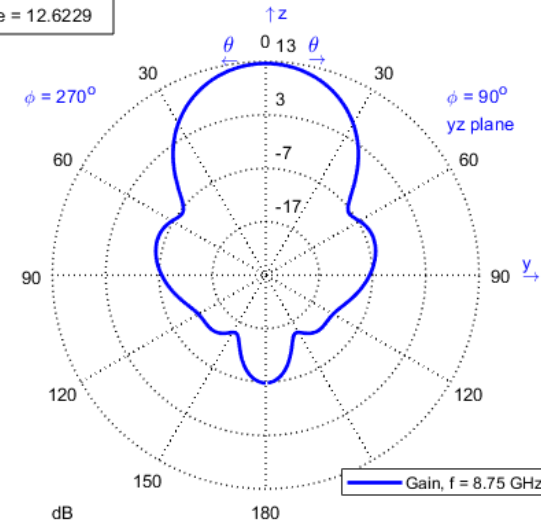
maximum value = -7.5093



maximum value = 12.6229

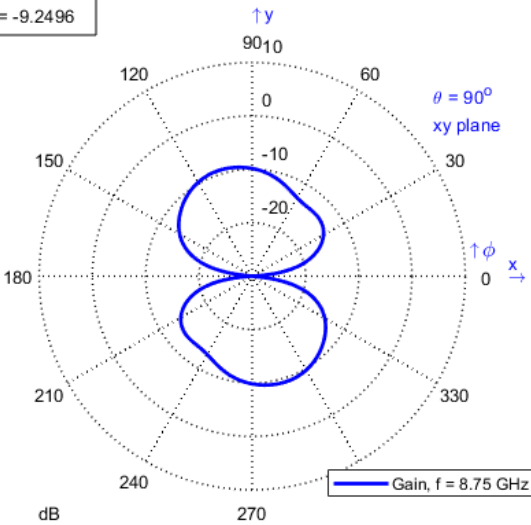


maximum value = 12.6229

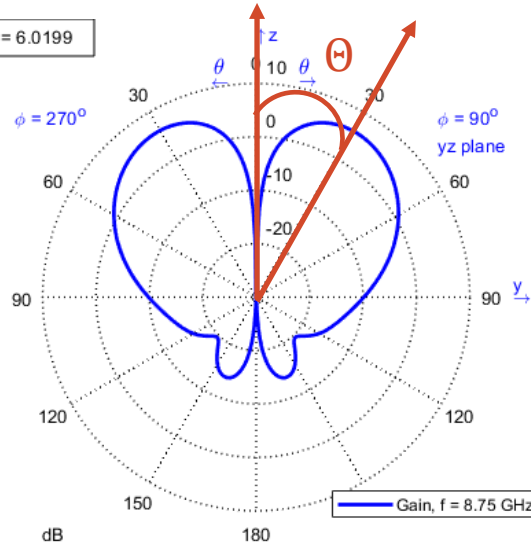


OAM mode 1

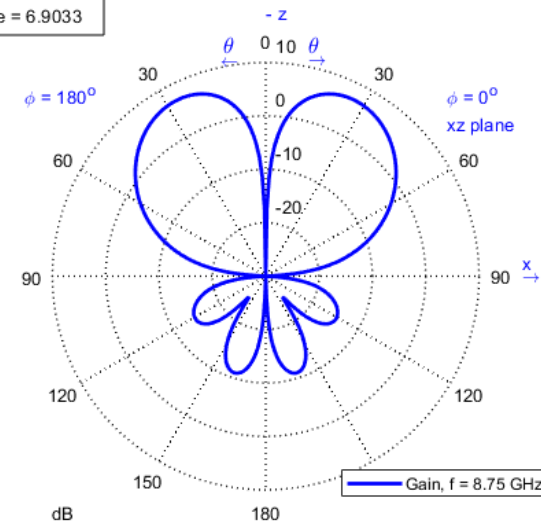
maximum value = -9.2496



maximum value = 6.0199

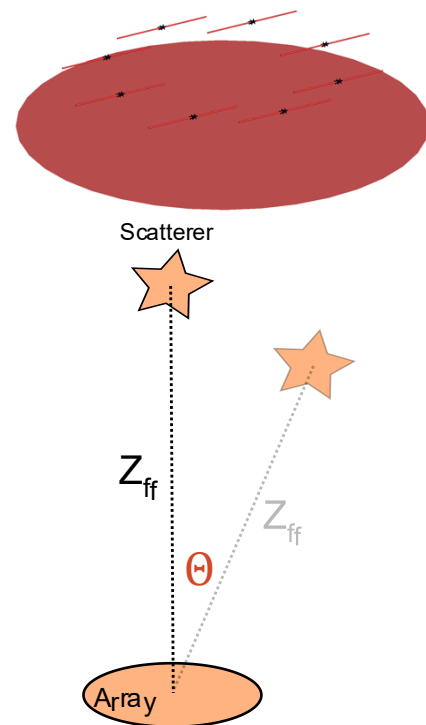


maximum value = 6.9033



$\Theta = 30^\circ$ Divergence Angle

Scatterers will be placed in the main radiation lobe at the far field boundary as illustrated

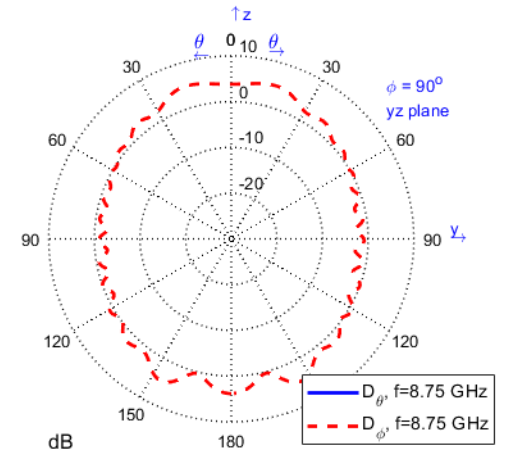
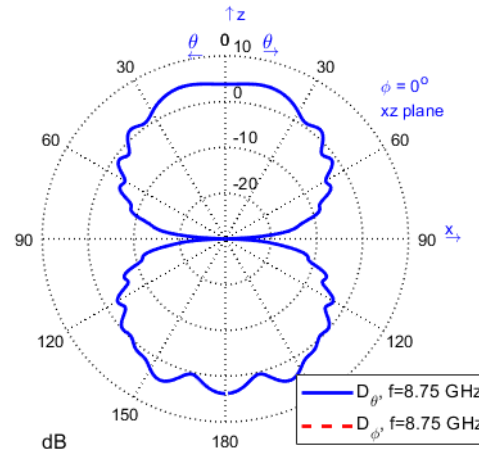
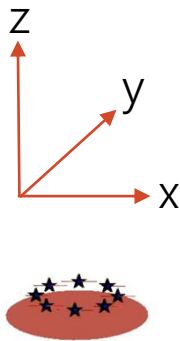
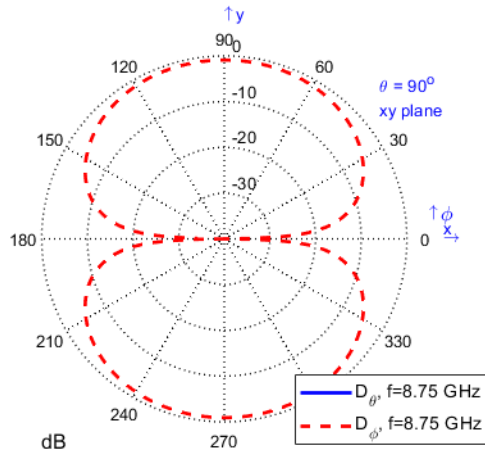


Simulation: Scattered Field Results

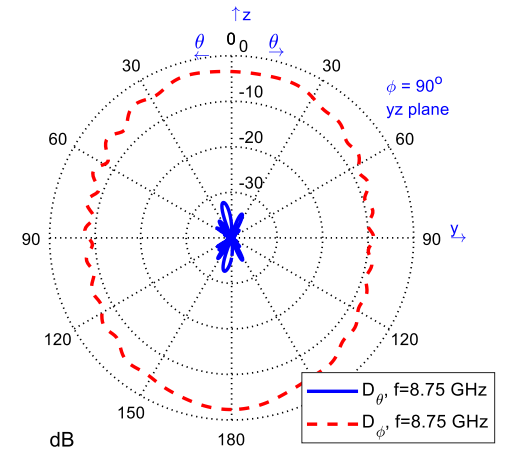
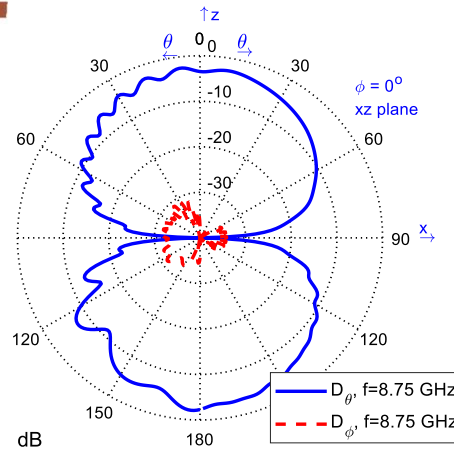
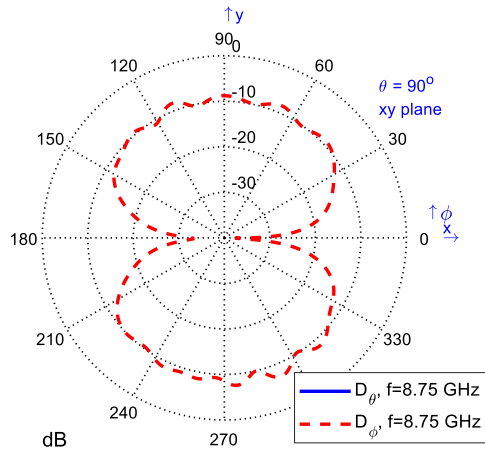
Scattering directivity is reported normalized to scattered power from the plane wave incidence

$$D = \frac{4\pi U}{P_{scattered,pw}}$$

OAM mode 0



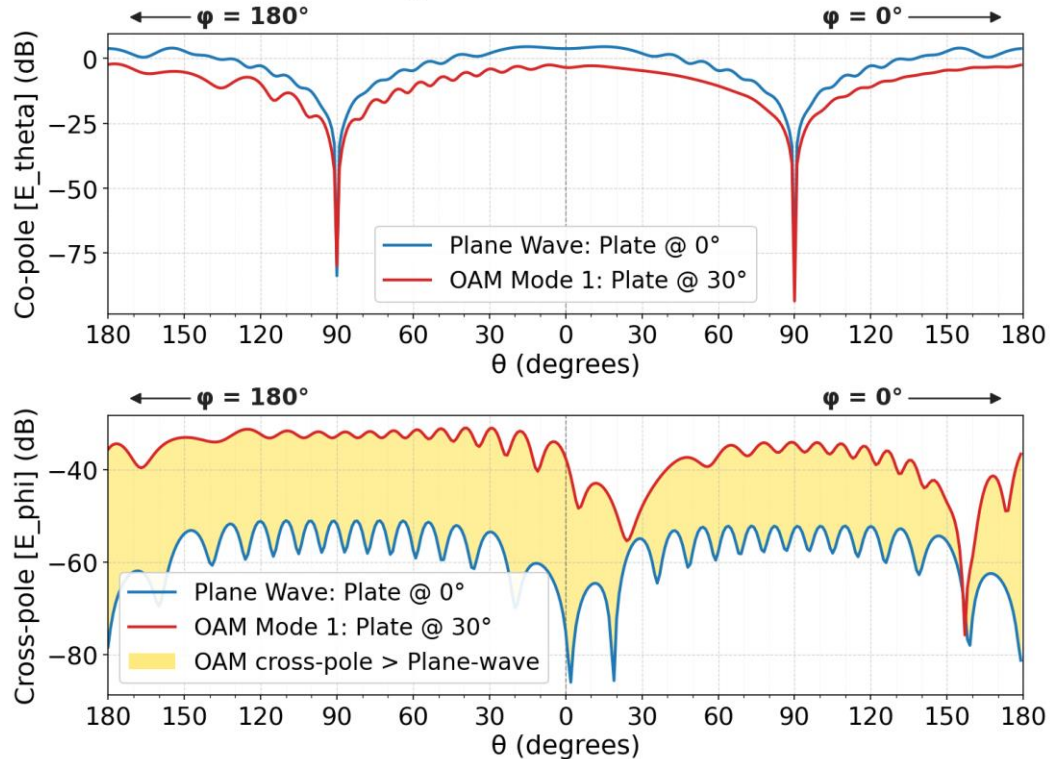
OAM mode 1



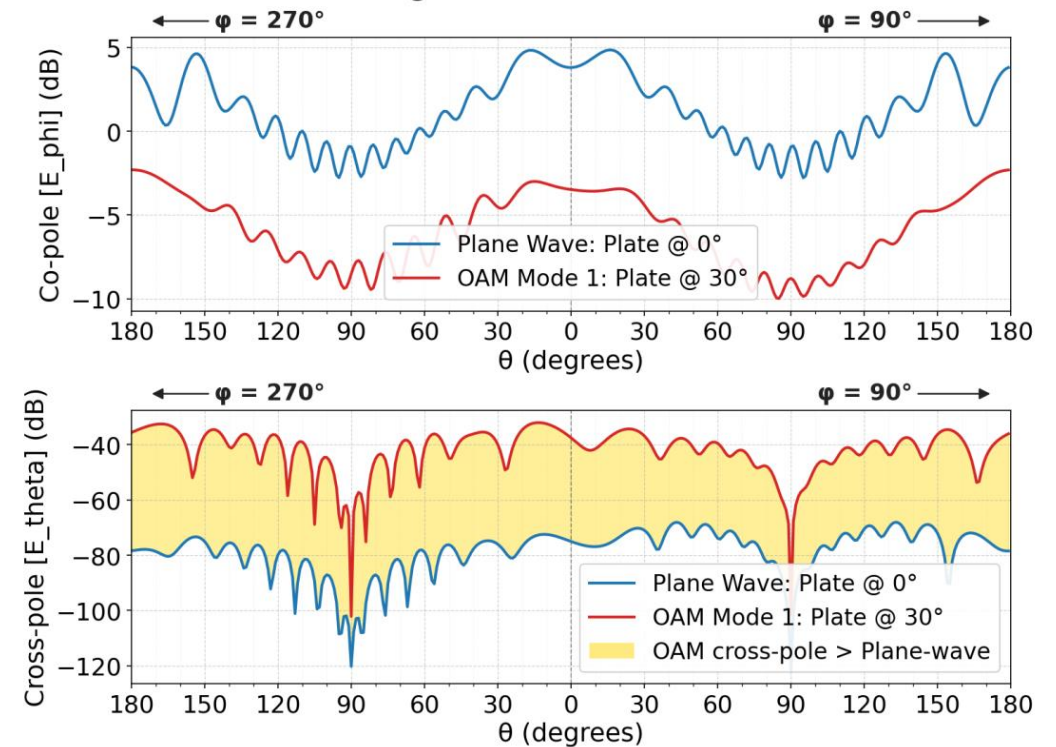
Simulation: Scattered Field Results

The co-polarized scattering is very similar, but there is much more cross-polarized scattering for structured illumination

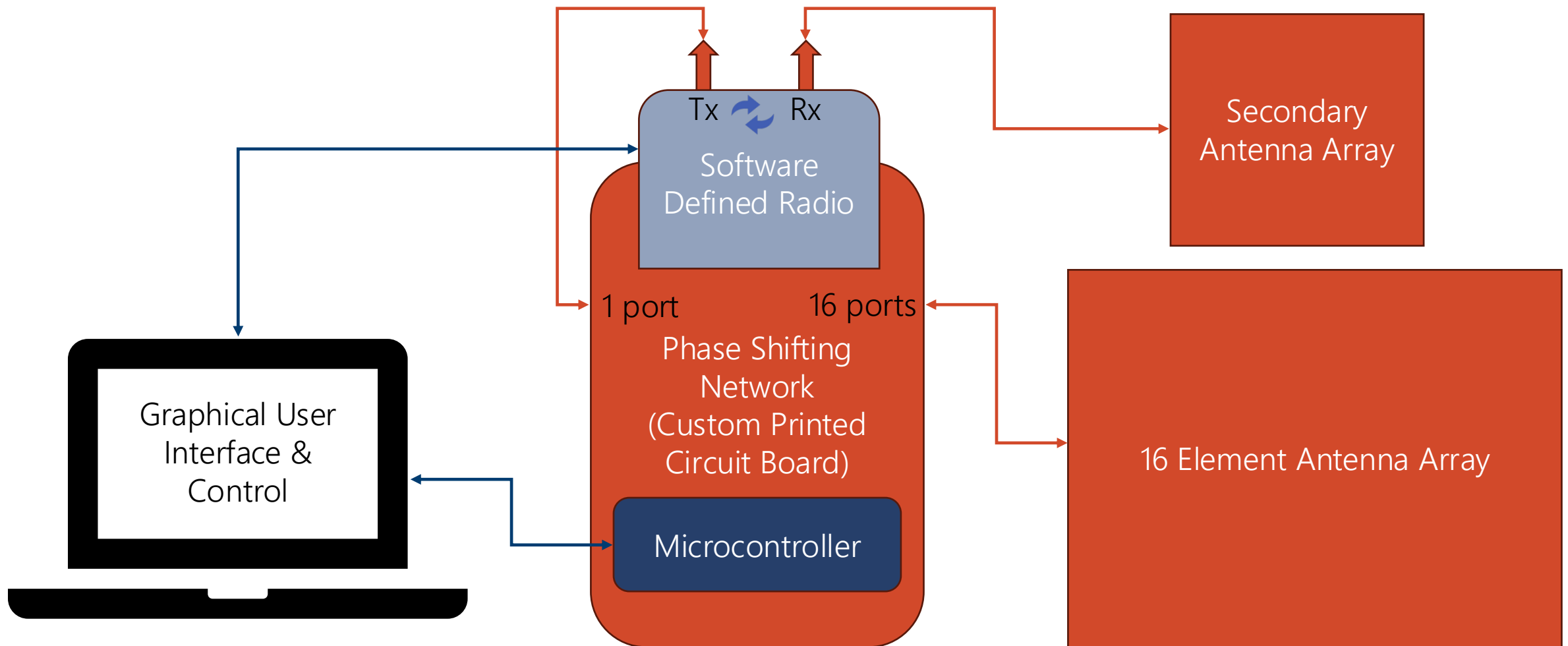
XZ Cut — Scattering Comparison
Plane Wave Illumination: Plate @ 0° vs OAM Mode 1: Illumination Plate @ 30°



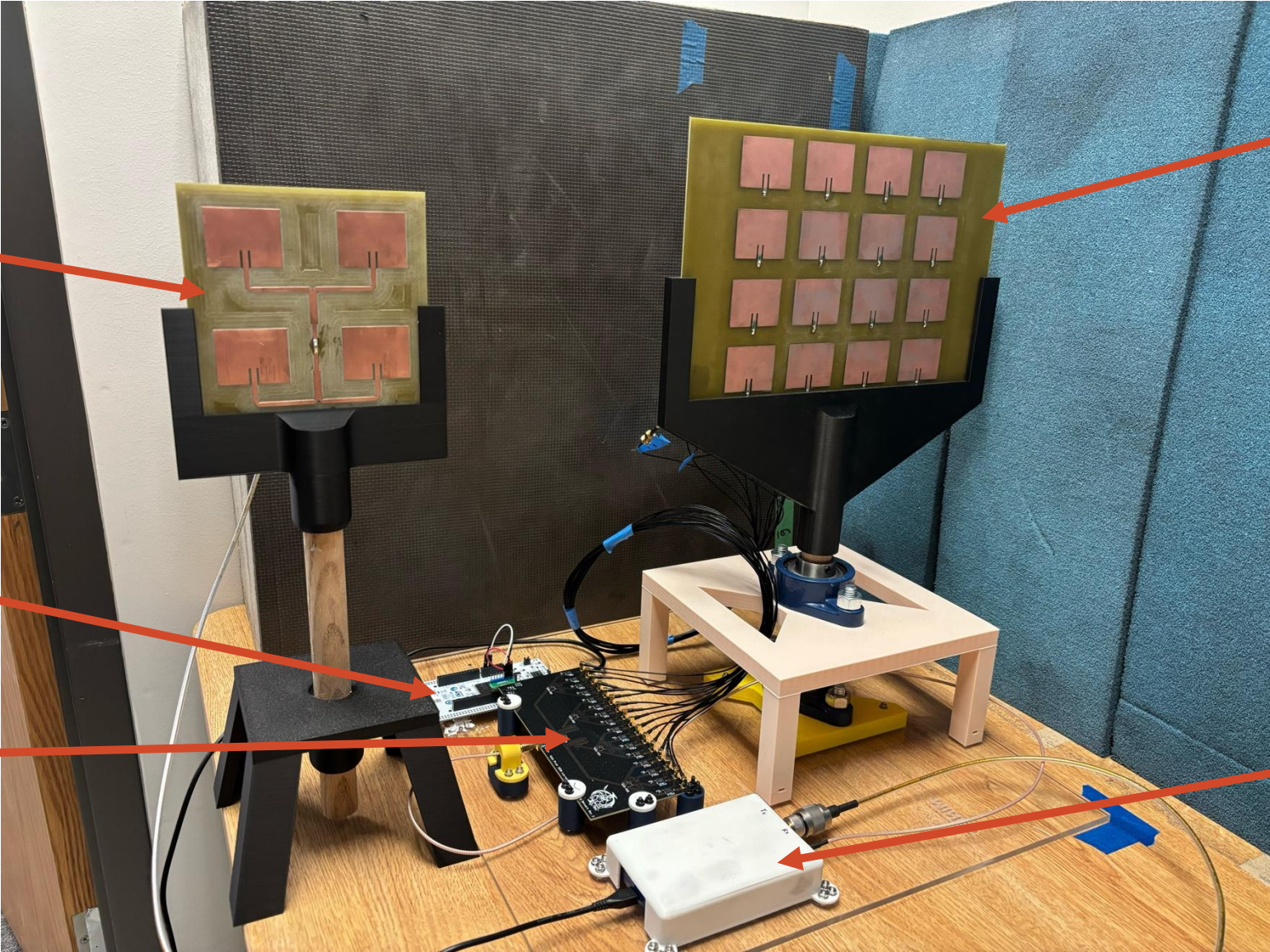
YZ Cut — Scattering Comparison
Plane Wave Illumination: Plate @ 0° vs OAM Mode 1: Illumination Plate @ 30°



Phased Array Experimental System Design



Components of the Designed Phased Array System



Secondary
Antenna Array

Primary Antenna
Array

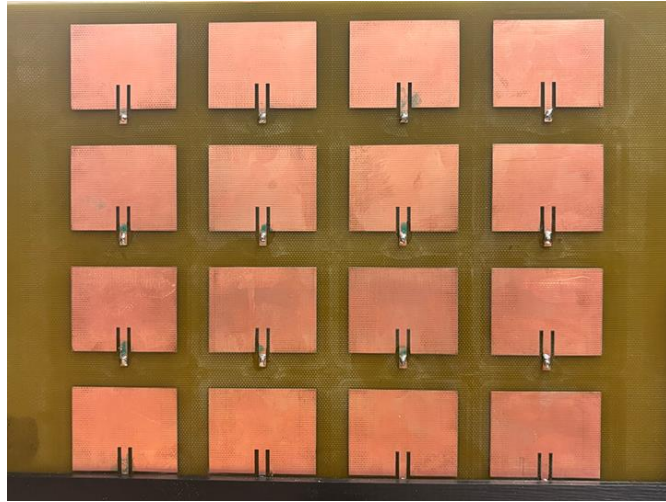
Microcontroller

Custom Phase
Shifting Network

Software Defined
Radio

Primary and Secondary Arrays Performance

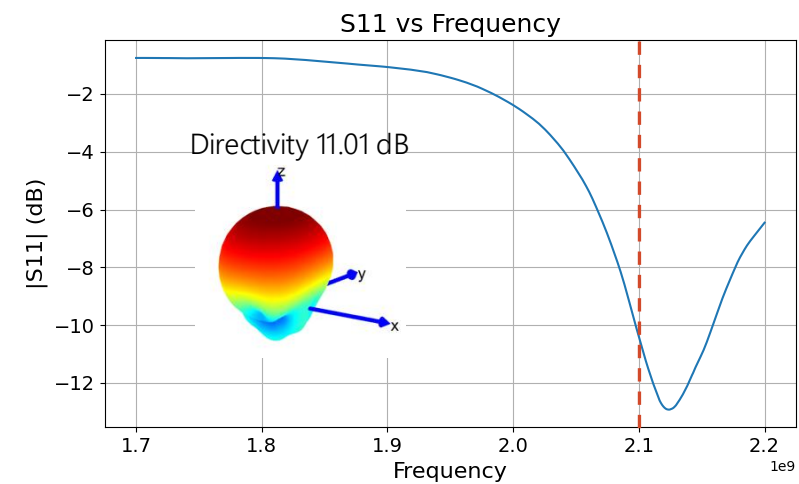
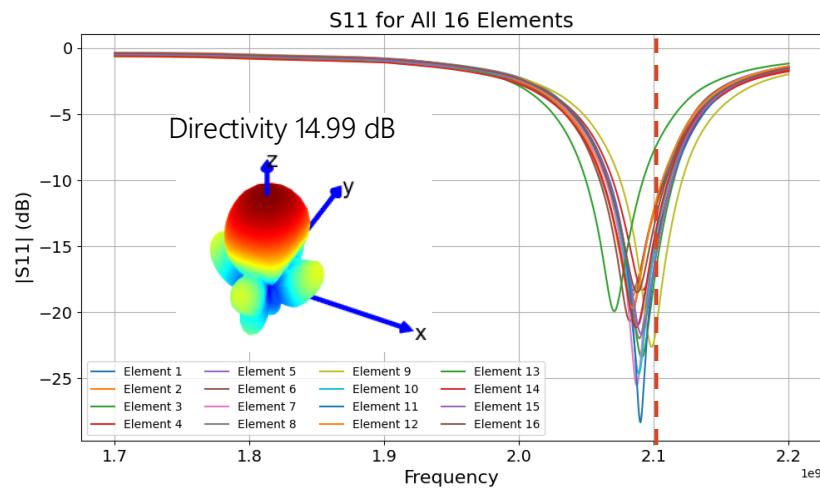
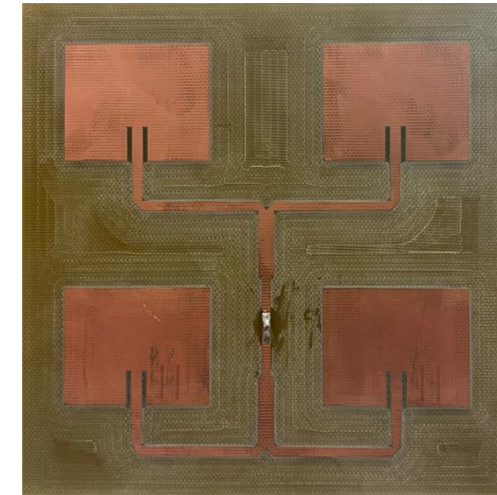
Primary



Simulation Results using CEMS

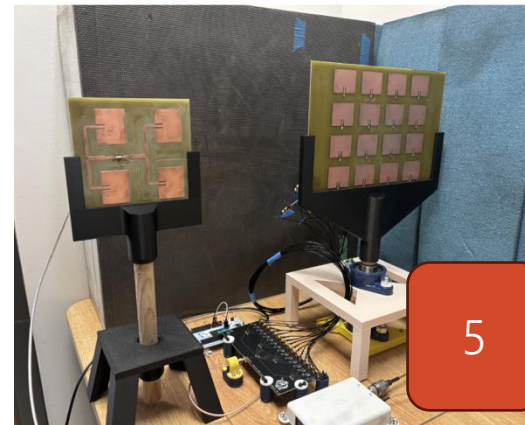
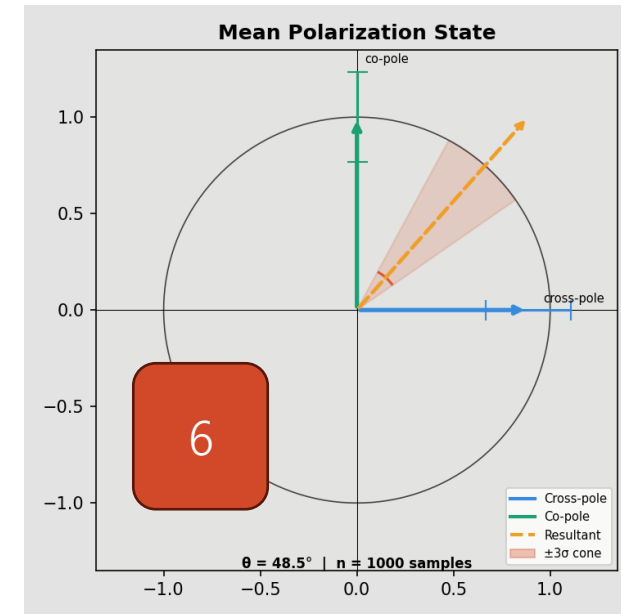
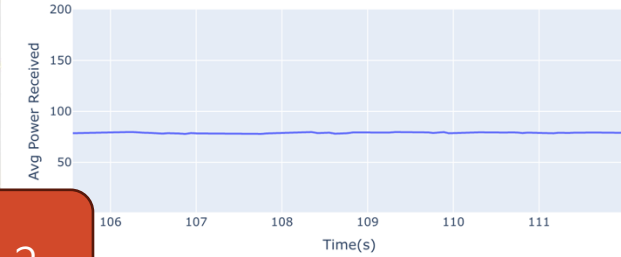
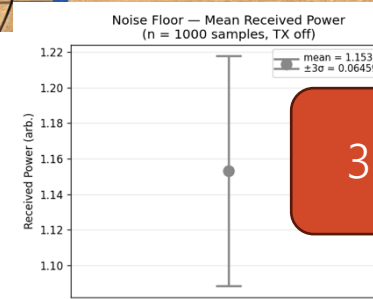
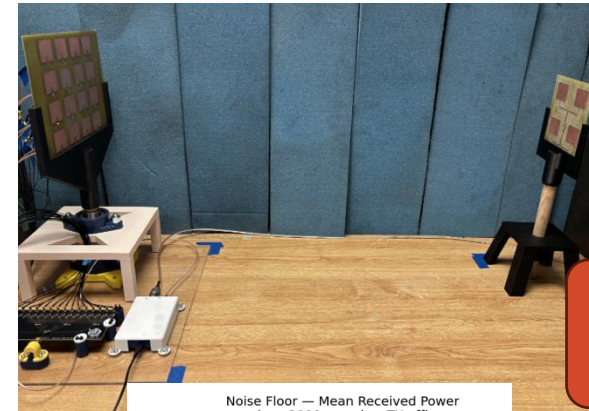
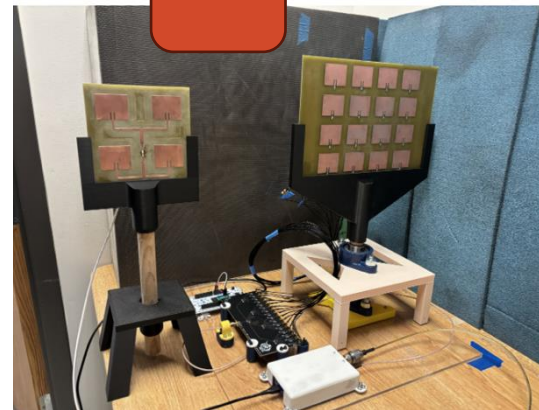
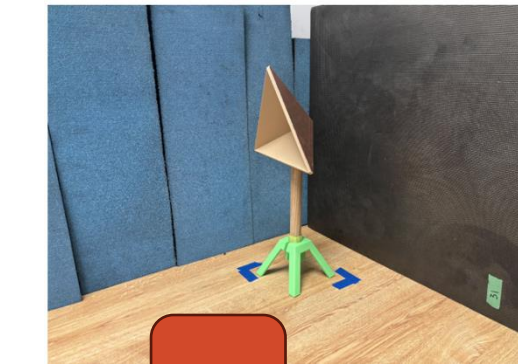
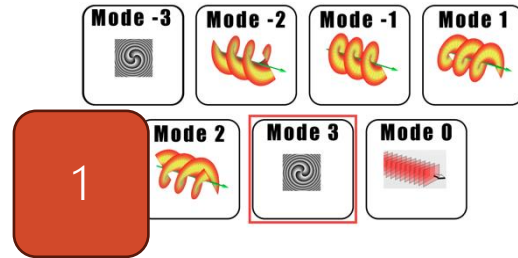
Measured Input Reflection Coefficient

Secondary



Measurement Procedure – 6 Steps

1. Mode Selection: Plane Wave or Structured Beam
2. Define Main Beam Direction
3. Measure System Noise
4. Measure Co-Polarized Scattering
5. Measure Cross-Polarized Scattering
6. Report Return Polarization State



Power Measurements

To measure system noise (Step 3), co-polarized scattering (Step 4), and cross-polarized scattering (Step 5) the following method is applied:

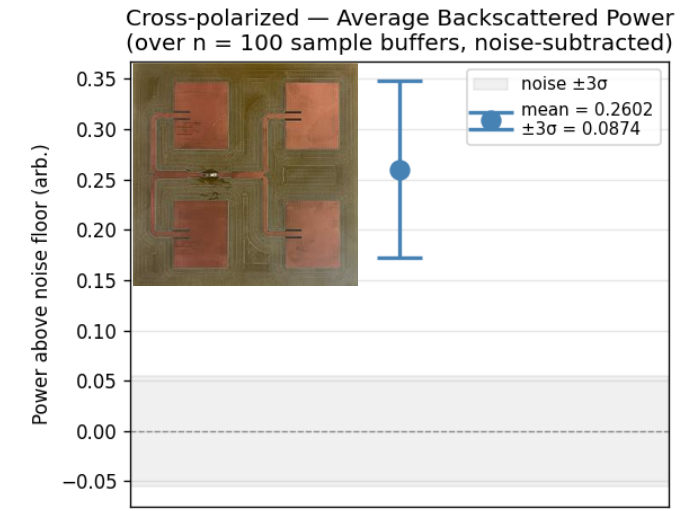
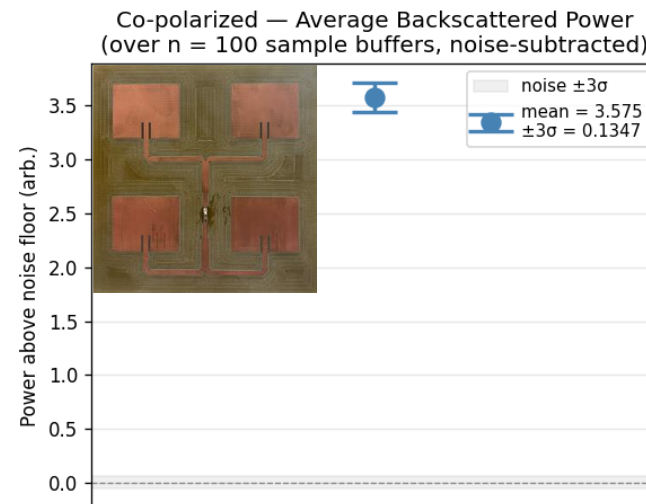
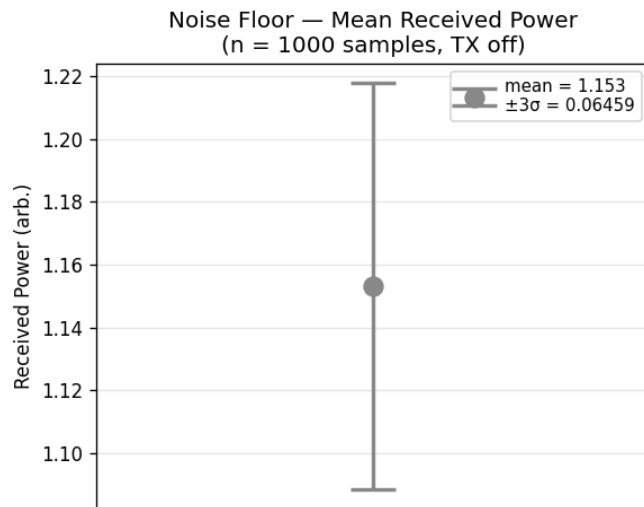
The instantaneous power given a complex sample $x = I + jQ$ is given as $|I + jQ|^2$ the average power is then given as:

$$\mu = \frac{1}{N} \sum_{n=0}^{N-1} |x[n]|^2$$

Where N is the length of the sample buffer = 8192

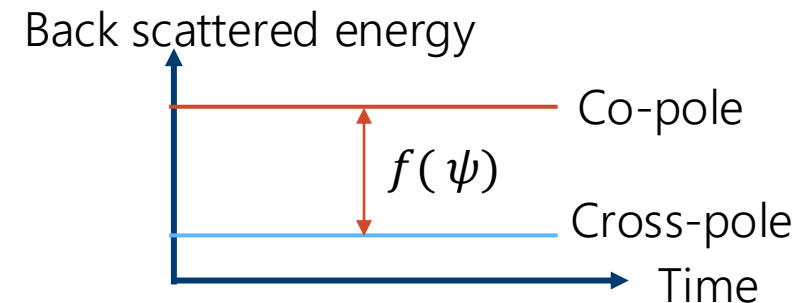
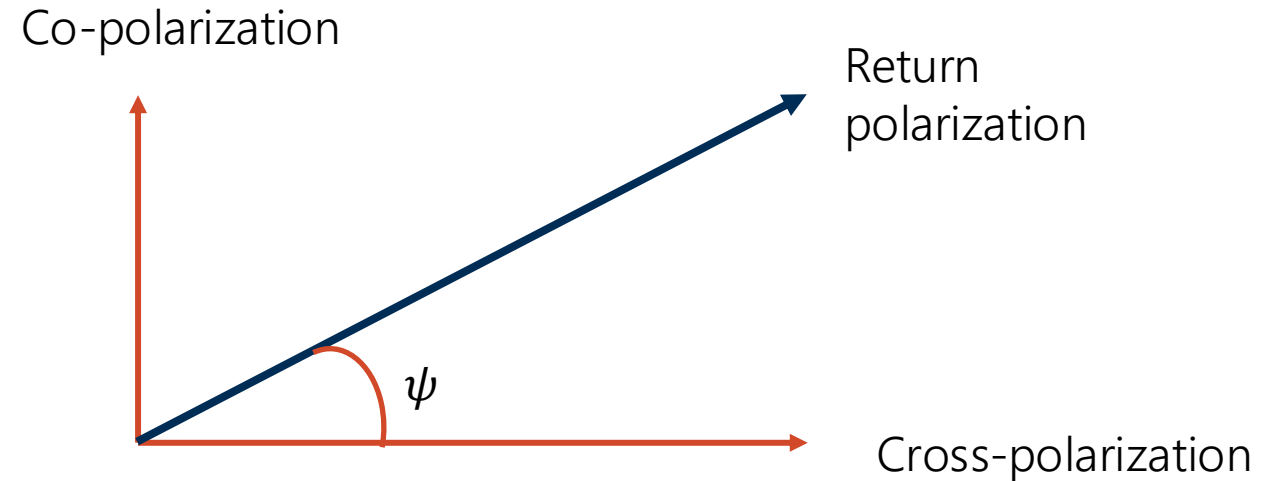
It should be noted that the power units are *arbitrary*, as they are derived from raw ADC samples from the software-defined radio.

The mean μ is computed for 100 sample buffers and the standard deviations σ of these means are reported to generate a 3σ confidence interval (99.7%)



Effective Polarization State (Step 6)

- To quantify the energy scattered we can break it into co-polarized and cross-polarized components and report the effective polarization vector
- Then the angle between the cross-polarized and effective polarization vector tells us to what degree scattering polarization changes
- $\psi = 90^\circ$ polarization preserved
- $\psi = 0^\circ$ complete shift in polarization
- This quantity is helpful to illustrate differences in structured beam scattering and planewave scattering.



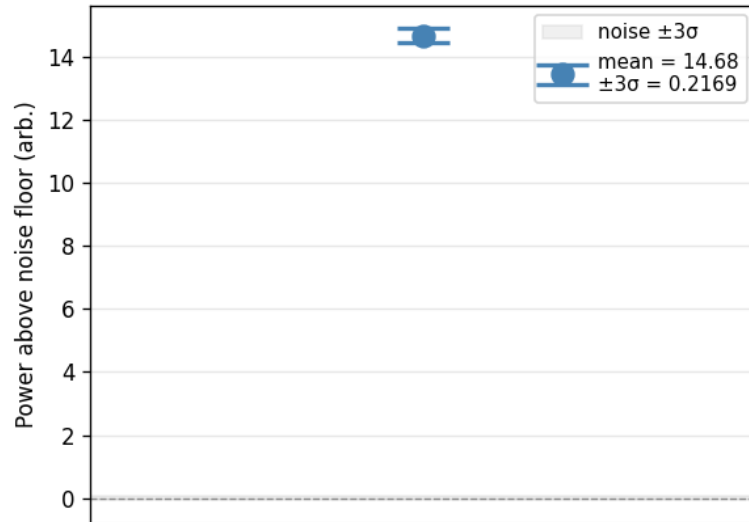
Experimental Results with Plane Wave Excitation

To mirror the simulated experiment a 7x7 cm copper plate was used as the scatterer with side length equivalent to the $\frac{\lambda}{2}$ at 2.1 GHz.

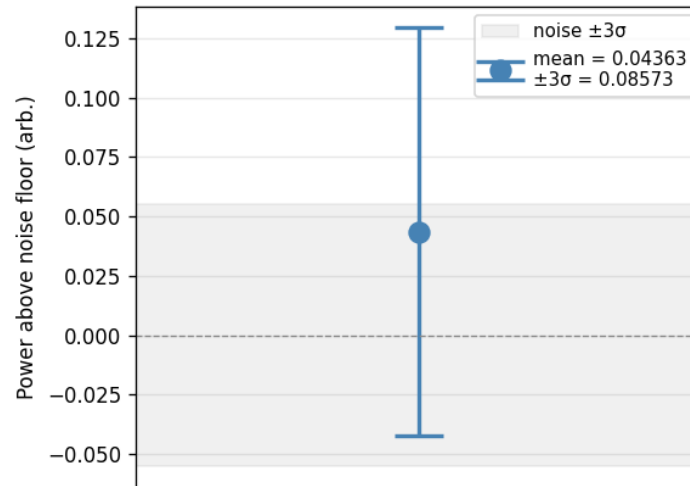
Under Plane wave illumination



Co-polarized — Average Backscattered Power (over n = 100 sample buffers, noise-subtracted)



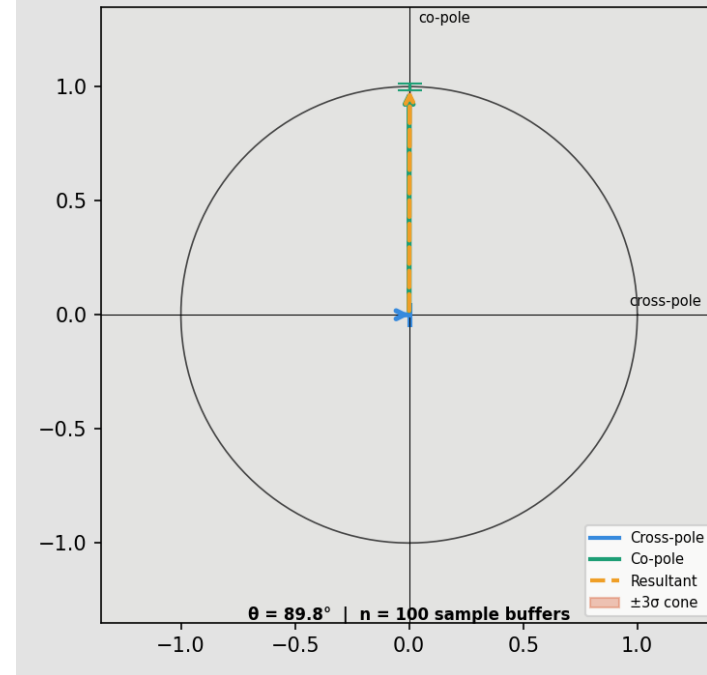
Cross-polarized — Average Backscattered Power (over n = 100 sample buffers, noise-subtracted)



Virtually no cross-polarized scattering

$\psi \approx 90^\circ$

Mean Scattered Polarization State



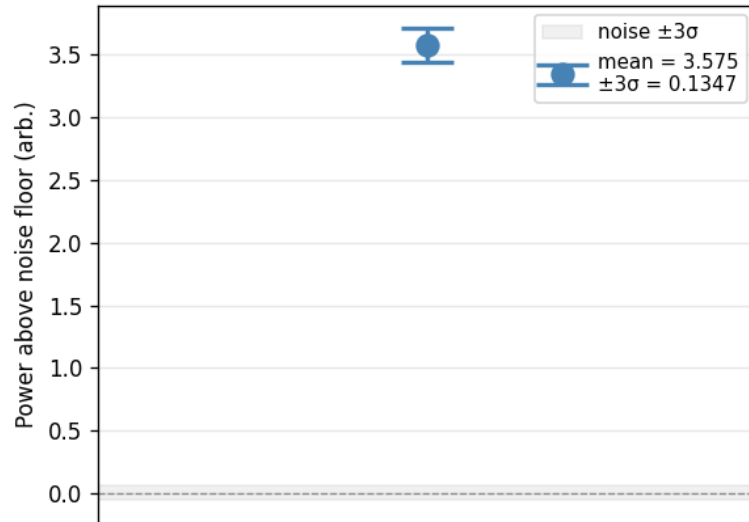
Experimental Results with OAM Beam Excitation

The same 7x7 cm copper plate was used as the scatterer with side length equivalent to $\frac{\lambda}{2}$ at 2.1 GHz.

Under OAM Mode 1 Illumination



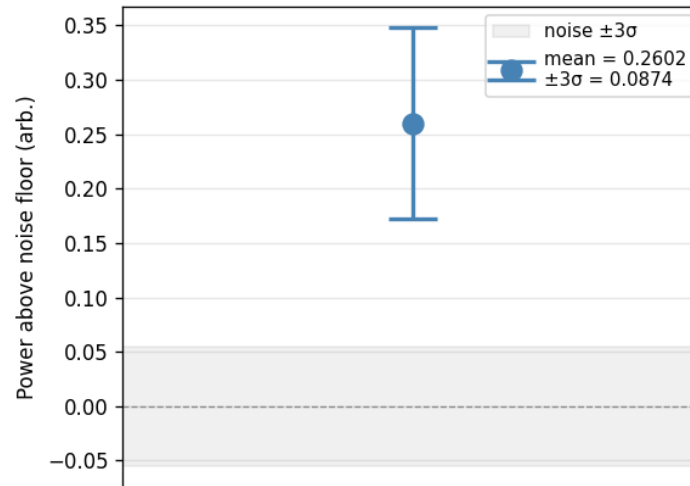
Co-polarized — Average Backscattered Power (over n = 100 sample buffers, noise-subtracted)



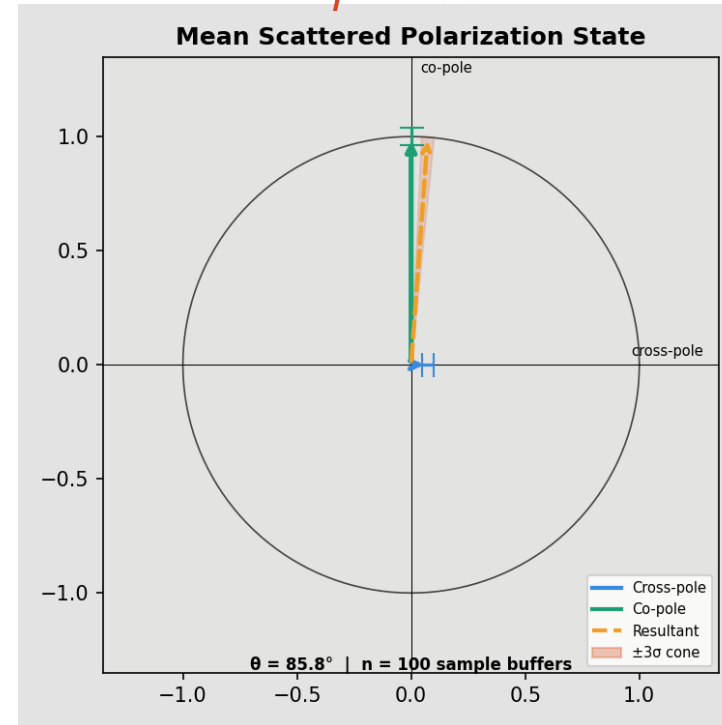
Lower backscattered power because of beam divergence (see slide 9)

Relevant cross-polarized scattering

Cross-polarized — Average Backscattered Power (over n = 100 sample buffers, noise-subtracted)

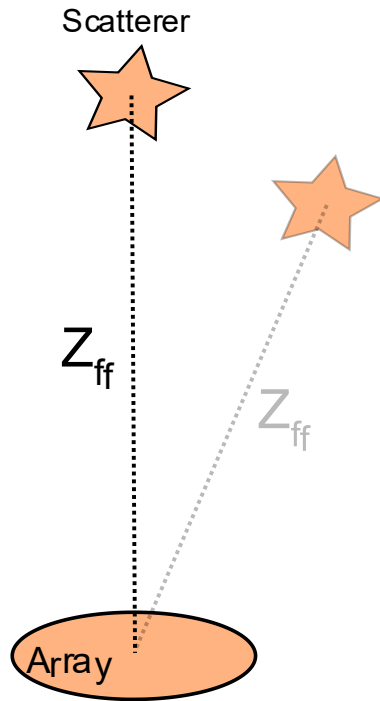


$\psi \approx 86^\circ$

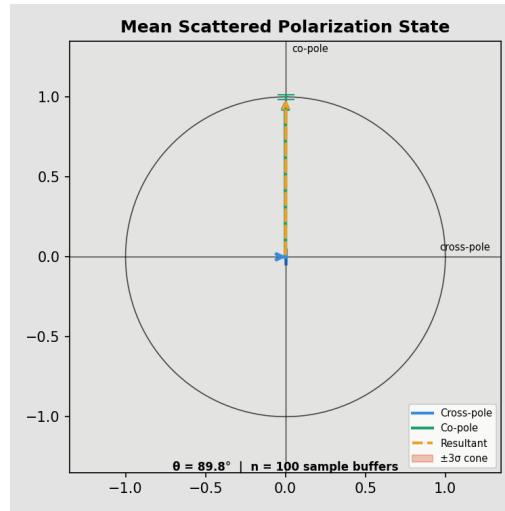


Plane Wave and OAM Beam Scattering Comparison

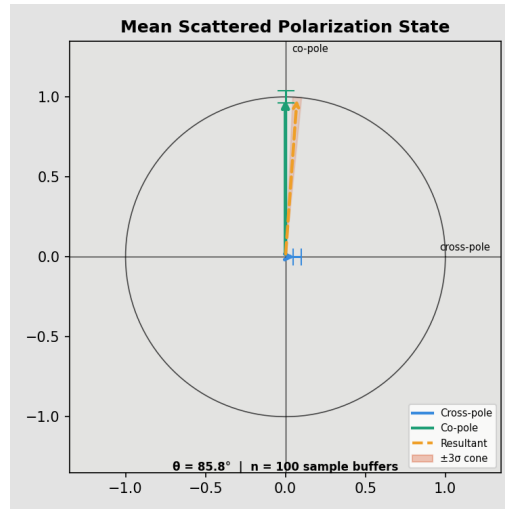
Key observation: Cross-polarized scattering from incident structured waveforms exceed their plane-wave counterpart



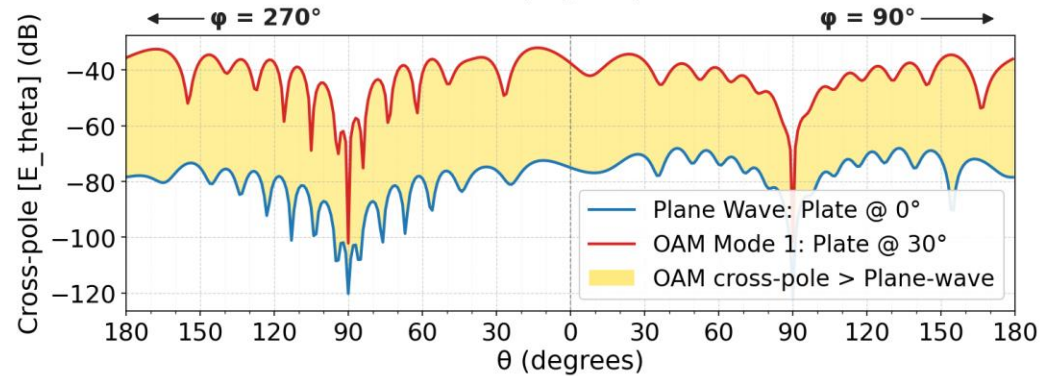
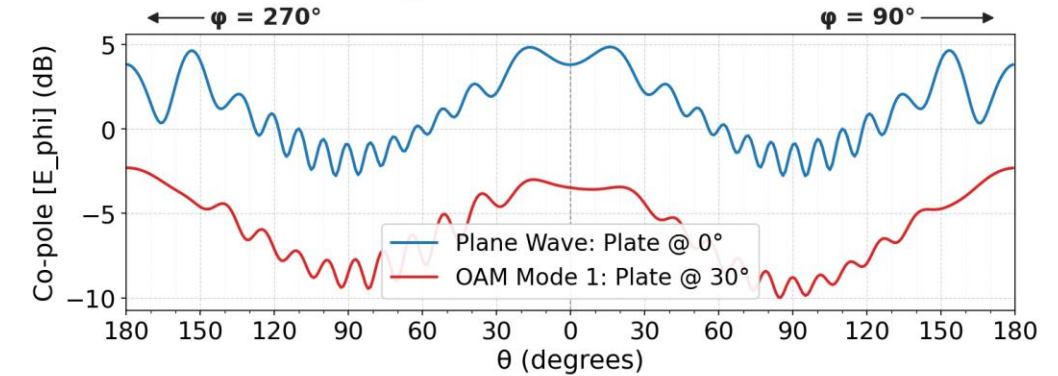
Plane Wave



OAM Beam



YZ Cut — Scattering Comparison Plane Wave Illumination: Plate @ 0° vs OAM Mode 1: Illumination Plate @ 30°



Conclusion

- A complete polarimetric scattering analysis was conducted for a PEC plate using simulation and experimentally using a custom phased array hardware-software testbed setup
- Results suggest that structured beams produce a cross-polarized scattering component larger than the one produced when using plane waves
- This polarimetric diversity in scattering can be leveraged to enhance existing radar solutions, particularly for target classification and imaging.

Future Work

- Since the investigation of beams carrying orbital angular momentum is of interest, examining scattering from rotating targets may provide insightful results.
- Research in the optical domain has shown a way to characterize targets' angular momentum by illuminating them with OAM beams, and this can be further examined [2].
- Exciting multiple OAM modes simultaneously due to their orthogonal property could add to the target's scattering characteristics [3].
- Development of different antenna arrays to optimize the mode purity of each orbital angular momentum mode [4].

References

- [1] A. Elsherbeni and V. Demir, *The finite-difference time-domain method for electromagnetics with MATLAB® simulations: ACES series, 2nd edition*. 01 2016, pp. 1–531.
- [2] M. Lavery, F. Speirits, S. Barnett, and M. Padgett, 'Detection of a Spinning Object Using Light's Orbital Angular Momentum', *Science*, vol. 341, pp. 537–540, 08 2013.
- [3] T. Yuan, H. Wang, Y. Qin, and Y. Cheng, 'Electromagnetic Vortex Imaging Using Uniform Concentric Circular Arrays', *IEEE Antennas and Wireless Propagation Letters*, vol.15, pp.1024-1027, 2016.
- [4] D. Liu, W. Wu, L. Gui, and T. Jiang, 'OAM mode purity improvement based on antenna array', *Digital Communications and Networks*, vol. 10, no. 4, pp. 1145–1153, 2024.
- [5] T. Yuan, Y. Cheng, H.-Q. Wang, and Y. Qin, 'Generation of OAM radio beams with modified uniform circular array antenna', *Electronics Letters*, vol. 52, no. 11, pp. 896–898, 2016.

Questions?

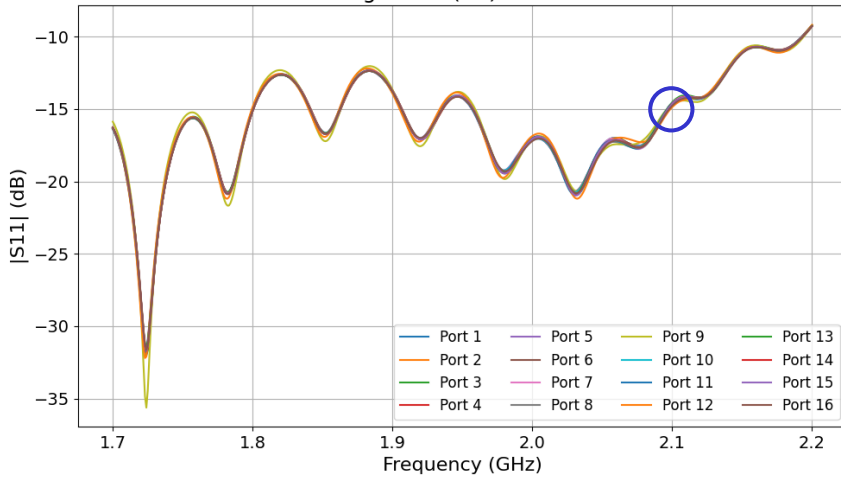
Electrical Engineering Department,
Colorado School of Mines, Golden, CO 80401, USA
<https://arc.elsherbeni.com>



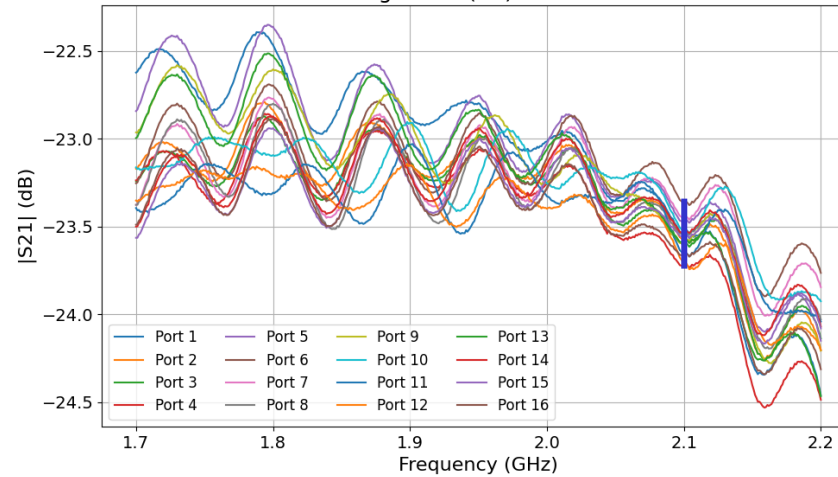
Backup Slides

16 Ports Scattering Parameters

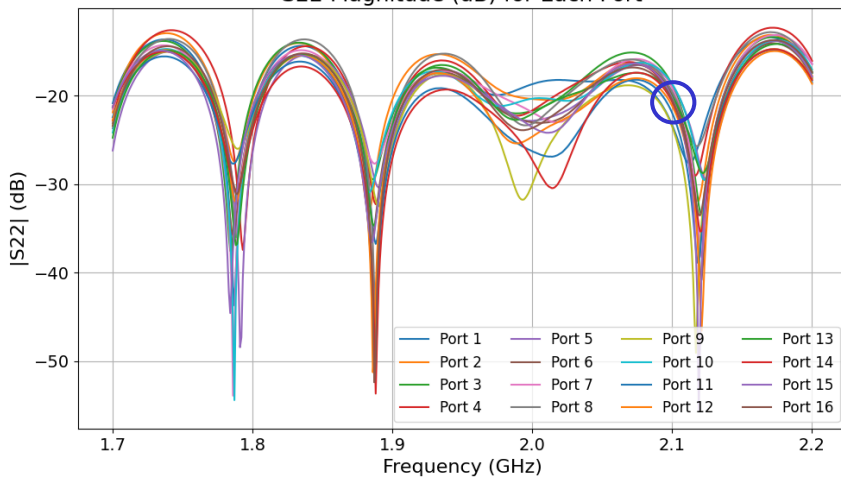
S11 Magnitude (dB) for Each Port



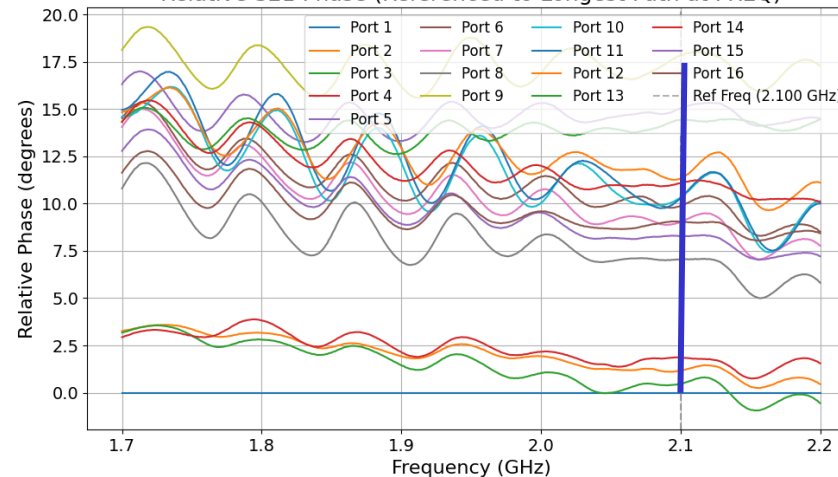
S21 Magnitude (dB) for Each Port



S22 Magnitude (dB) for Each Port



Relative S21 Phase (Referenced to Longest Path at FREQ)



@2.1 GHz

- Insertion loss difference is maximum of 0.5 dB
- Maximum phase difference of 17.5 degrees (to be calibrated to have 0 phase difference with software)
- S11 and S22 at all ports are all at the same level

Calibration Process

- Determine the largest phase offset
- Compute the difference in phase and store them into *phase_offsets* variable
- Before sending phases to the microcontroller, adjust the phase offsets of each element to coincide with the largest phase offset.
- This is all automated in the graphical user interface, which generates the required calibration

